Soft-Synchronization of Generators Using Controllable Inductive Fault Current Limiters

Yucheng Zhang, *Member, IEEE*, and Roger A. Dougal, *Senior Member, IEEE*

***Abstract*—We describe a method for soft-synchronization of generators by controlling an inductive fault current limiter located between the generator and the grid. Our method limits the peak shaft torque and the frequency oscillations that normally occur following mistimed closure of the bus tie switch. The method improves the success rate of generator close-in, especially during emergencies or when operating with low transient-stability margin, with low inertia and, therefore, it lengthens the life of turbogenerators. This method introduces no adverse effects during an ideal (correctly timed) generator-synchronization process. We prove the success of the technique by using transient time-domain analysis and describe the control and an approach to analyze the soft-synchronization process that can be generally applied to either an infinite power system or to a limited-capacity system. After the generator is synchronized to a grid and operates stably, the transient-stability margin between the generator and the grid is not affected by this method. This soft-synchronization method has been validated by simulations with the increased critical margin of the rotor-angle difference and the improved faulty synchronization process with limited power impulse and frequency oscillation.**

***Index Terms*—Fault current limiters (FCLs), synchronization, synchronous generators.**

I. Introduction

DUE TO the rapid expansion of capacity in electric power systems, larger available fault currents may cause the existing circuit breakers (CBs) to become underrated. Fault current limiters (FCLs) can eliminate this problem by limiting currents during faults [1], [2]. FCLs can be installed at generator feeders to limit fault currents from the generator site [3]. In some circumstances, generators must be frequently synchronized into or removed from the grid. So it is important to ensure a fast and reliable synchronization process. When bringing generation online, turbogenerators, transformers, and associated equipment can be damaged if a bus tie connects two systems when they are not yet synchronized. High peak currents and off-frequency operation can cause winding stresses, high rotor iron currents, pulsating torques, and mechanical resonances that are potentially damaging to the machine [4]. If not outright damaged, these poor synchronizations lead at least to loss of equipment [5]. Faulty synchronizations, those that have a rotor-angle difference δ that is not nearly zero at the moment of closing the bus tie, can be caused by slow or variable speed of mechanical movement of bus ties, and the improper tripping of controllers and associated equipment [6]. Although an "out of step" relay can detect loss of synchronization and isolate the affected generator [7], this method for handling the problem adversely affects the supply of power during emergencies, just when power may be the most needed.

Besides limiting fault currents, controllable FCLs can also help maintain generator synchronization. In this paper, we propose the control of the soft-synchronization process with the application of controllable inductive FCLs. The parameters of controllable inductive FCLs can be defined by users in a certain range during the manufacturing process [8], [9]. And the principle of this soft-synchronization process is analyzed with the help of a transient-stability margin plot [10]–[12]. The simulations verifying this method can be generally applied in an infinite power system and an isolated power system. In this method, the controllable inductive FCLs are installed at generator terminals to offer a soft and reliable generator synchronization process.

II. Controllable Inductive FCLs and Soft-Synchronization Process

A. Controllable Inductive FCLs

An FCL is a variable-impedance device that is connected in series with a power circuit to limit the system current under fault conditions. It has low impedance (ideally negligible impedance) under normal operating conditions and high impedance (not infinite) under fault conditions. Many kinds of FCLs have been developed over the past several decades [1], [2]. These can be classified into three main groups depending on their fundamental technology: 1) superconducting FCLs [13], [14]; magnetic FCLs [15]; and solid-state FCLs [16]. Alternatively, classification by impedance is possible, in which case the main classes are inductive FCLs and resistive FCLs. Due to less heat dissipation and lower requirements on cooling systems, we have considered only inductive FCLs, not resistive FCLs, in this paper.

For the study in this paper, we have developed a generic performance model with appropriate parameterization. This generic performance model is intended to represent the inductive FCL device, which inserts or removes an in-series inductance within a certain time, regardless of the activation mechanism.

Manuscript received October 01, 2010; revised January 25, 2011 and April 07, 2011; accepted May 08, 2011. Date of publication June 23, 2011; date of current version October 07, 2011. This work was supported in part by the U.S. National Science Foundation under Grant 0652271 and in part by the Office of Naval Research under Grant N00014-08-1-0080. Paper no. TPWRD-00754-2010.

The authors are with the Department of Electrical Enginnering, University of South Carolina, Columbia, SC 29208 USA (e-mail: zhang22@cec.sc.edu; dougal@cec.sc.edu).

Color versions of one or more of the figures in this paper are available online at http://ieeexplore.ieee.org.

Digital Object Identifier 10.1109/TPWRD.2011.2156434

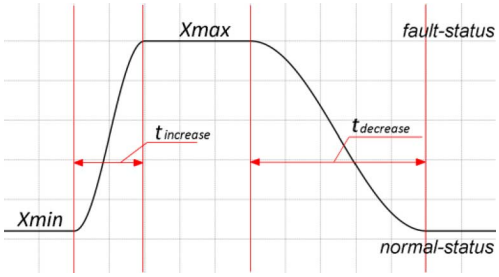

Fig. 1. Transient impedance of controllable inductive FCLs during a full operational cycle including activation time (t_{increase}), operating time in fault status, and reset time (t_{decrease}).

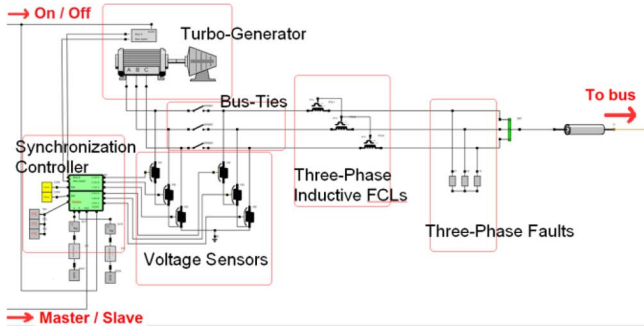

Fig. 2. One power generating unit in detail.

The particular medium-voltage inductive FCL device that we have chosen to study is bistable. (It is stable in the high and low inductance states.) It can be commanded at will to change states, and the change from state to state is a continuous function of time, as shown in Fig. 1.

The inductance of such a controllable FCL depends on its control signal. The control initiates a change in the device's inductance which has two steady-state values: $L_{\min}$ and $L_{\max}$. After a transition is commanded, L changes continuously from one of these limits to the other, along some trajectory that we have chosen to represent here as a smooth cosine function. (This could have been a linear function, or any other math function, but the nuances of the change are relatively immaterial to the system performance.) The inductance during the rise time is then described by (1), shown at the bottom of the page, and the inductance during the fall time is described by (2), shown at the bottom of the page.

In these equations, $\Delta L = L_{\max} - L_{\min}, t_{\text{increase}}$ is the time to transition from $L_{\min}$ to $L_{\max}, t_{\text{decrease}}$ is the time to transition from $L_{\max}$ to $L_{\min}, t_{\text{trigger}}$ defines the instant at which the inductance increase is irrevocably triggered, and t_{reset} defines the instant at which the inductive FCL is commanded to reset, and the inductance begins to decrease.

Fig. 1 shows the curves of increasing and decreasing FCL inductances, which simulates the changing inductance curves of a "Cryo-Pinch" superconducting FCL [8]. In this FCL device, an actuator moves some piece of the magnetic circuit in order to change the inductance. The actuator consists of a motor driven by power-electronics devices and communication circuits. There are immense forces acting on the magnetic components, and the mechanism moves the inductance smoothly along some trajectory from $L_{\min}$ to $L_{\max}$ (or from $L_{\max}$ to $L_{\min}$) when no current is flowing through the FCL device. During fault current limitation, there is feedback between the forces created by the fault current and the forces created by the actuator mechanism. So the trajectory of inductance will be somewhat different when current is flowing because of the forces created by the fault current. But for the soft-synchronization study in this paper, the flowing current starts from zero and is much smaller than the fault current, which is typically tens of norminal current, during the inductance-changing period. The force created by the flowing current is very small and negligible. So the model developed here is suitable for the soft-synchronization study in this paper.

The default values of this model, shown in the Appendix, are consistent with those of the "Cryo-Pinch" superconducting FCL. It is noted that the reset time (t_{decrease} >10 ms) can be defined by adjusting the setting of the microprocessor in the actuator of the FCL device [8]. The FCL device has a range of inductance of 0.1 to 0.3 mH in a prefault mode and when in a current limiting mode, the inductance changes to 5 to 15 mH for an inductance ratio of 50:1. While the results presented here will be typical, of course, other inductance ratios, such as 20:1, 40:1, or 60:1 will produce somewhat different results.

B. Principle and Analysis on the Soft-Synchornization Process

The synchronization process is realized by an automatic synchronizer. One power generating unit in detail is shown in Fig. 2.

After the turbogenerator reaches the steady state (voltage and frequency close to the reference values), the automatic synchronizer gives the speed and voltage reference bias to make:

- the frequency of the turbogenerator be slightly higher than the frequency of the grid;

$$L(t) = \begin{cases} L_{\min} & t < t_{\text{trigger}} \\ L_{\min} + \frac{\Delta L}{2}\left(1 - \cos\left(\frac{\pi(t - t_{\text{trigger}})}{t_{\text{increase}}}\right)\right) & t_{\text{trigger}} < t < (t_{\text{trigger}} + t_{\text{increase}}) \\ L_{\max} & t > (t_{\text{trigger}} + t_{\text{increase}}) \end{cases} \quad (1)$$

$$\cdots$$

$$L(t) = \begin{cases} L_{\max} & t < t_{\text{reset}} \\ L_{\max} + \frac{\Delta L}{2}\left(\cos\left(\frac{\pi(t - t_{\text{trigger}})}{t_{\text{decrease}}}\right) - 1\right) & t_{\text{reset}} < t < (t_{\text{reset}} + t_{\text{decrease}}) \\ L_{\min} & t > (t_{\text{reset}} + t_{\text{decrease}}) \end{cases} \quad (2)$$

$$\cdots$$

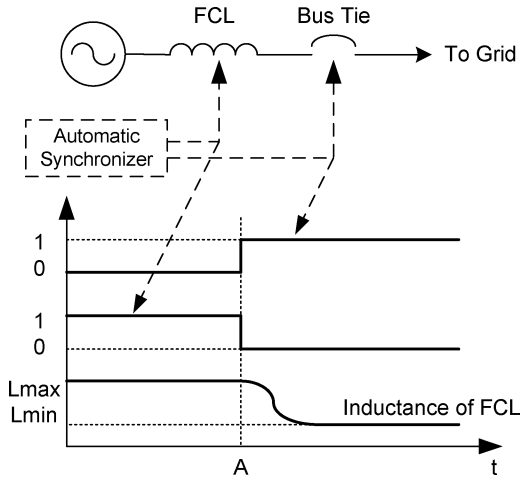

Fig. 3. Control signals of FCL and bus tie in the soft-synchronization method.

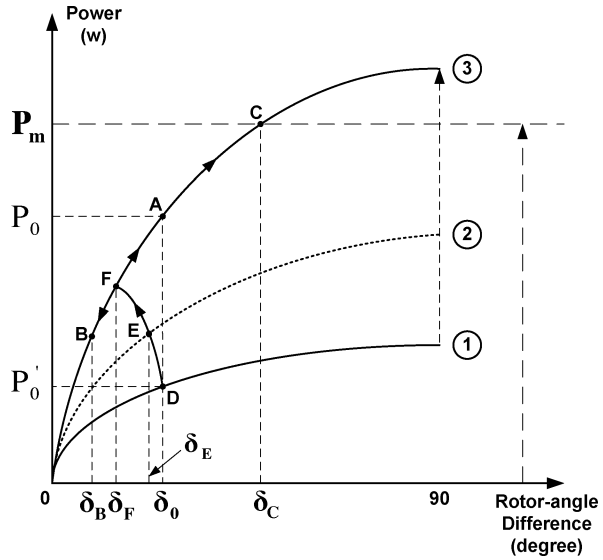

Fig. 4. Electrical power of the generator versus rotor angle for transient analysis.

- the terminal voltages across the bus tie have the same magnitude.

When 1) the frequency difference reaches the offset and remains stable; 2) the voltage difference is zero; and 3) the phase difference is zero, the automatic synchronizer triggers the bus tie to close. If these conditions are not satisfied, the synchronization process is not perfect and the soft-synchronization process is needed.

The soft-synchronization process starts with the bus tie open and the FCL in the high inductance mode. Immediately after closure, the FCL is commanded to reset to the low inductance mode so that its inductance decreases to the nominal working value, following (2). The command signals of FCL and the bus tie are presented in Fig. 3, where the generator is synchronized to the grid at point A.

Since the intended purpose of an FCL is to limit currents during fault conditions, we have worked within the current-limiting parameters in order to extend the operating mode to the soft-synchronization process. $L_{\max}$ and t_{increase} are determined by the maximum allowed fault current and the speed with which that current should be limited. We have set t_{decrease} in a range of 20–30 cycles (0.33 s–0.5 s for 60 Hz) which is long enough for the soft-synchronization process and yet does not adversely affect the reclosing of CBs in typical electric power systems.

The soft-synchronization process can be analyzed with the help of Fig. 4. In an ideal and classical synchronization process, the generator is synchronized to the grid so that the initial rotor-angle difference δ is " 0 ." When the bus tie is closed and the generator becomes loaded, the rotor angle increases to " δ_c." The generator operating point moves along the track "*0-B-F-A-C*" on curve-3. Curve-3 is the electrical power output of the generator without FCLs during transients, as (3). But in a faulty synchronization process, the bus tie is closed when the rotor-angle difference is not zero. The generator transfers a power impulse to the grid immediately when the bus tie is closed, shown as P_0 in Fig. 4, which imposes a large torque on the generator shaft which is followed by persistent torque oscillations that can shorten the life of turbogenerators. After closure of the bus tie, the mechanical output of the turbine engine increases from 0 to P_m—managed by the speed governor— while the operating point follows the track "*A-F-B-F-A-C*" on curve-3 during a dynamic oscillation process. Depending on the magnitude of the power impulse, δ_B may become negative. If the transient-stability margin is big enough, the generator may temporarily go into "motor-mode," and then pull back into "generator-mode" and perhaps oscillate this way several times. If damped, then finally, the generator becomes stably synchronized with the grid. On the other hand, if the transient stability margin is low, the oscillations between the motoring and generating modes may be underdamped so that a stable operating mode cannot be recovered

$$p_3 = \frac{V_{\text{Gen}}V_{\text{Grid}}}{X_d' + X_{\text{sys}}}\sin\delta \approx \frac{V_{\text{Gen}}V_{\text{Grid}}}{X_d' + X_{\text{sys}} + 2\pi f L_{\min}}\sin\delta \tag{3}$$

$$p_1 = \frac{V_{\text{Gen}}V_{\text{Grid}}}{X_d' + X_{\text{sys}} + 2\pi f L_{\max}}\sin\delta \tag{4}$$

$$p_2 = \frac{V_{\text{Gen}}V_{\text{Grid}}}{X_d' + X_{\text{sys}} + 2\pi f L_{\text{FCL}}(t)}\sin\delta \tag{5}$$

where

p_1, p_2, and p_3	electrical power of the generator during transients;
V_{gen}	internal voltage of the generator;
V_{grid}	system (reference) voltage of the grid;
X_d'	transient reactance of the generator;
X_{sys}	equivalent system reactance;
δ	rotor-angle difference between V_{gen} and V_{grid};
$L_{\text{FCL}}(t)$	transient inductance of FCLs during the soft-synchronization process, which satisfies $L_{\min} < L_{\text{FCL}}(t) < L_{\max}$.

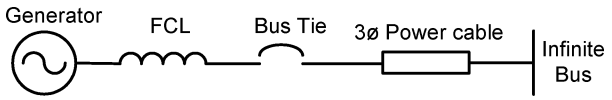

Fig. 5. Topology of one DG synchronizing to an infinite bus.

When applying this soft-synchronization process, the rotor angle starts from δ_0 too. But the transient power impulse following closure of the bus tie is decreased to $P_0^{'}$, which is much smaller than P_0. Curve-1 is the electrical power of the generator with FCLs at $L_{\max}$ as (4), and curve-2 is the electrical power during the changing-inductance period of FCLs as (5). The operating point moves along the track of "*D-E-F-A-C*." It should be noted that the track of " $D-E-F$ " is dynamically influenced by the changing inductance of the FCL, tracking of the turbine governor, the net inertia of the turbogenerator, and associated system parameters. The transient-stability margin of the generator changes from the value associated with curve-1 to that associated with curve-3, while the inductance of FCL decreases from $L_{\max}$ to $L_{\min}$.

By applying the soft-synchronization process with controllable inductive FCLs, the power impulse can be decreased from P_0 to $P_0^{'}$ at the instant of closing the bus tie. Also, the system oscillation can be limited during the synchronization process. After the generator is synchronized to the grid and runs stably, the FCL stays at $L_{\min}$ and the transient-stability margin between the generator and the grid is not affected by the installation of FCLs.

III. Simulation Results

Two series of simulations were performed to verify the operation of this soft-synchronization method. The first considered one turbogenerator connected to an infinite grid, while the second one considered two similar turbogenerators of similar capacity working in an isolated power system. Details of these models and their parameters are provided in the Appendix.

A. One Generator Synchronizing to an Infinite Bus

Here, we analyze the case of connecting a single distributed generator (DG) into an infinite bus. The circuit is shown in Fig. 5. A three-phase FCL is installed to limit the generator's contribution to fault currents so that the existing protection relay scheme for the rest of the system continues to be sufficient. Two common conditions aggravate the synchronization process by reducing the stability margin—high impedance between the generator and the infinite grid and low inertia of the DG. Therefore, we analyze the high-impedance, low-inertia case in particular. The grid is modeled as an ideal voltage source in series with a reactance of 0.38 ω.

In an ideal synchronization process, the phase of the DG is drifted slowly across the phase of the grid and the bus tie is closed exactly at the instant of zero phase error. Since the loaded phase is slightly different than the unloaded phase, minor oscillations in frequency and electrical power of the generator are excited, as shown in Fig. 6.

The transient-stability margin of the generator decreases with increasing line impedance to the grid. The improvement on the generator synchronization is validated by this case which has a long-distance power cable (0.5 p.u., based on the generator ratings) and a faulty synchronization process with $\delta_0 = 20°$. The total inertia constant of the gas turbogenerator is 2.0 s, which is near the lower bound of the normal range for thermal and hydraulic generating units [17]. This case has a low inertia in the turbogenerator, low transient-stability margin, and, therefore, a high requirement for precision in the synchronization process. The electrical power and frequency of the generator are compared between the two conditions with and without this soft-synchronization process, as shown in Fig. 7.

Without the soft-synchronization process, a large power impulse of 32 MW flows immediately after the bus tie closes, and

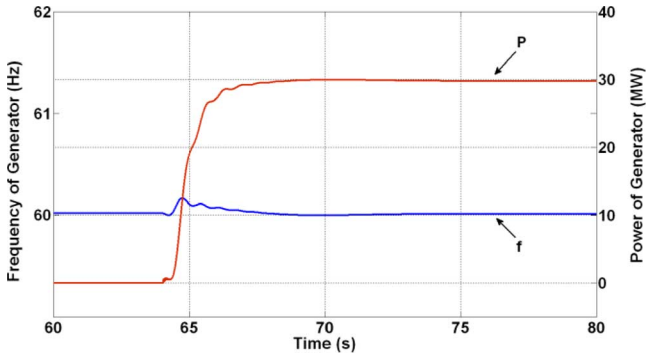

Fig. 6. Frequency and electrical power of the generator during an ideal synchronization process ($\delta = 0$).

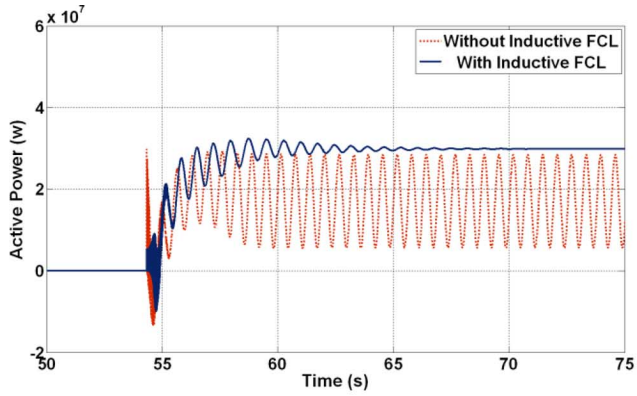

(a)

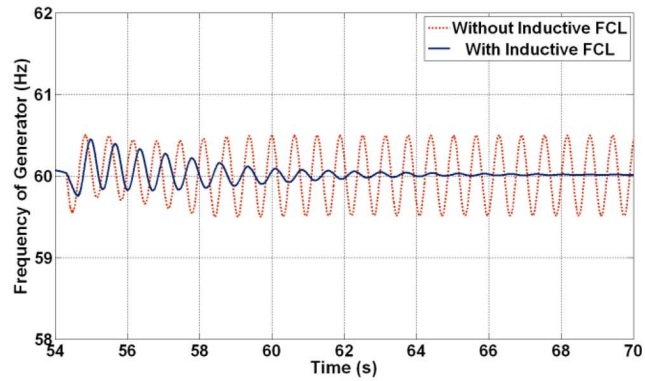

(b)

Fig. 7. Comparisons of frequency and electrical power of the generator between the conditions with and without the soft-synchronization process. (a) Electrical power of the generator. (b) Frequency of the generator.

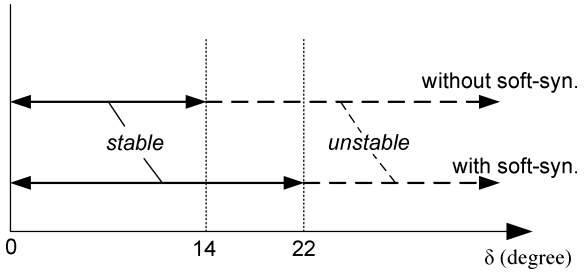

Fig. 8. Improvement of the success rate of faulty synchronizations by applying the soft-synchronization process.

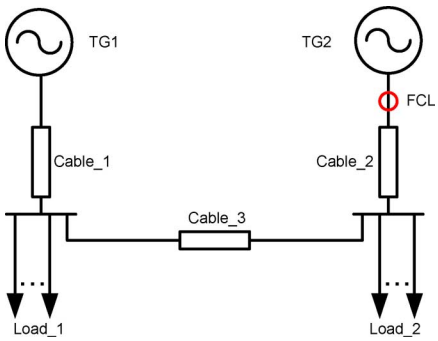

Fig. 9. Isolated power system with two 36-MW gas turbogenerators.

then the generator loses synchronism with the infinite bus. The large oscillations in power and frequency would result in an out-of-step relay removing the generator from the infinite bus, except that the effect is not represented in our simulation.

In contrast, applying the soft-synchronization process with the controllable inductive FCL installed, the power impulse following closure of the bus tie is limited to 5 MW. The active power of the generator gradually increases to the defined loading of 30 MW with some oscillations, and becomes stable after about 10 s.

A further series of simulations was conducted to identify the limiting rotor-angle difference that still ended in stable operation of the generator. We can see that the critical rotor-angle difference δ_0 increased from 14° without use of the soft-synchronization process to 22° by applying the soft-synchronization method, as shown in Fig. 8.

It is obvious and verified by our simulations that the generator synchronization performance can be improved by any of these methods: 1) increasing the transient-stability margin; 2) increasing the inertia of the turbogenerator; or 3) applying both of these methods. But the soft-synchronization method still benefits the faulty synchronization processes with a smaller power impulse and less frequency oscillation, both of which can lengthen the life of generators and improve the stability of the network. The results are similar to the ones in Section III-B with somewhat different values.

B. Generator Synchronization in an Isolated Power System

An isolated power system, such as in a small community or onboard a ship, differs from the semiinfinite grid by having lower inertia and higher impedance. So each generator can swing the entire grid and thereby influence the stability and

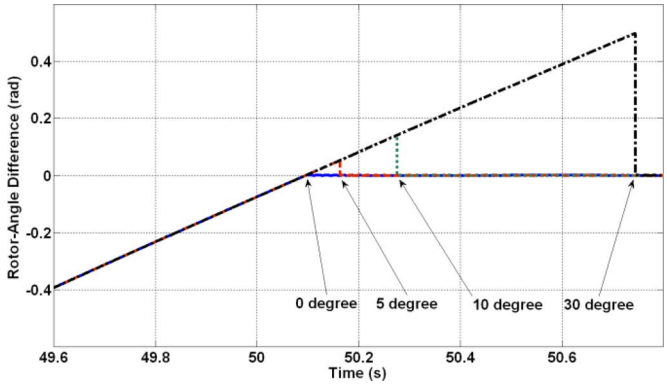

Fig. 10. Rotor-angle differences at the instant of closing the bus tie near TG2.

power quality of the entire system. In consideration of fuel economy, generators must be frequently synchronized into or removed from the grid as the load varies. The resulting heavy aging of switches may increase the number or severity of mistimed synchronizations.

We study the case of isolated power systems with the situation of two 36-MW turbogenerators that supply loads in a radial structure, as shown in Fig. 9. One generator (TG1) establishes the power supply first. Then, the second generator (TG2) is synchronized to the live grid and picks up a share of the load. We study two cases: in one case, the two generators are connected directly to the grid; and in the other case, a three-phase controllable inductive FCL is installed between TG2 and the bus so that the soft-synchronization process can be applied. A lumped R-L load of 24 MW ($\mathrm{PF} = 0.8$, lagging) is connected to the interconnected busses. Initially, only TG1 supplies electric power to the load of 24 MW. After TG2 is synchronized to TG1 and combined into the grid, the total load of 24 MW is shared equally by TG1 and TG2 (12 MW each) with TG1 operating in isochronous mode, and TG2 working in droop mode.

Here, we compare the synchronization processes for initial rotor-angle differences of 0°, 5°, 10°, and 30°. The initial rotor-angle difference δ_0 is defined as the rotor-angle difference at the instant of the closing bus tie, as shown in Fig. 10. The initial rotor-angle differences of 0° present an ideal synchronization process, and the ones of 5°, 10°, and 30° represent mistimed closures of the bus tie switch.

The frequency of TG1, which operates in isochronous mode reveals the transient stability of the grid while TG2 synchronizes into the isolated power system. The active power of TG2 represents the power impulse during synchronization. And the load voltage shows the power quality (voltage sag) during the synchronization process.

Fig. 11(a), (d), (g), and (j) compares the performance of the system with and without the FCL by plotting the frequency of TG1 for initial rotor-angle differences of 0°, 5°, 10°, and 30°. The frequency oscillations of the faulty synchronization processes are limited, and there are no complications for the ideal synchronization process ($\delta = 0°$).

Fig. 11(b), (e), (h), and (k) presents the power flow from TG2 at the first few cycles after the closure of the bus tie, with initial rotor-angle differences of 0°, 5°, 10°, and 30°. The power impulse during faulty synchronization is reduced by 50% with

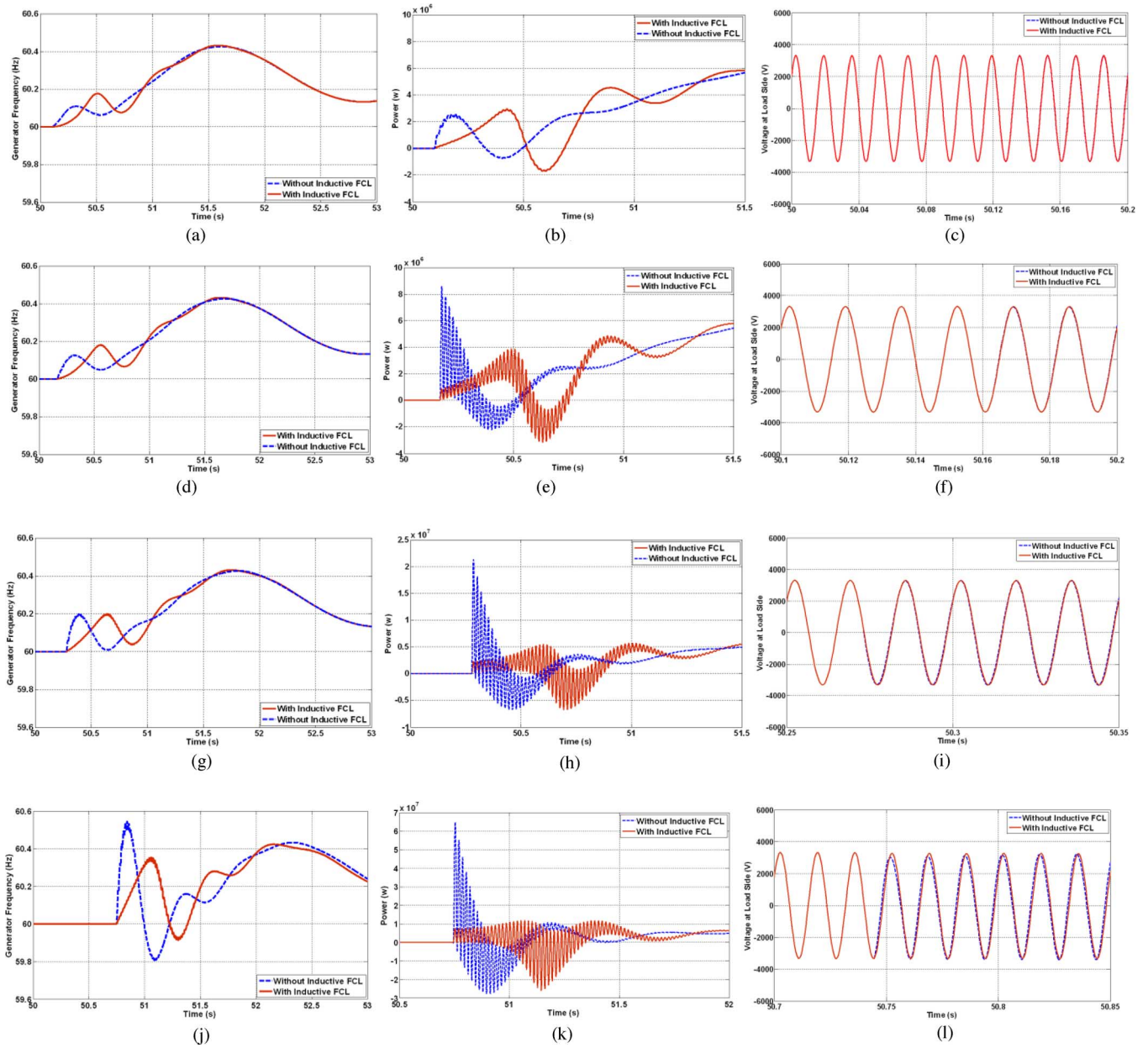

Fig. 11. Comparisons of frequency of TG1, active power of TG2, and voltage of loads, at $\delta = 0°$, 5°, 10°, and 30°, with and without the soft-synchronization process. (a) Frequency of TG1, at $\delta = 0°$, (b) Active power of TG2, at $\delta = 0°$. (c) Voltage of loads at $\delta = 0°$. (d) Frequency of TG1 at $\delta = 5°$. (e) Active power of TG2 at $\delta = 5°$. (f) Voltage of loads at $\delta = 5°$. (g) Frequency of TG1 at $\delta = 10°$. (h) Active power of TG2 at $\delta = 10°$. (i) Voltage of loads at $\delta = 10°$. (j) Frequency of TG1 at $\delta = 30°$. (k) Active power of TG2 at $\delta = 30°$. (l) Voltage of loads at $\delta = 30°$.

the soft-synchronization process. There is no aggravation on the ideal synchronization ($\delta = 0°$) by applying this soft-synchronization method.

Fig. 11(c), (f), (i), and (l) presents the effect of the soft-synchronization process on voltage sags at the load during the synchronization processes. It can be observed that there is no obvious voltage sag when the initial rotor-angle differences are 0° and 5°. But there is evident voltage sag for initial rotor-angle differences of 10° and 30°, without inductive FCLs installed. By applying this soft-synchronization method, the power quality on the buses is improved with lower voltage sag.

The data of these simulations are summarized in Table I. On the one hand, the soft-synchronization process does not influence the ideal synchronization process ($\delta = 0°$). On the other side, during the faulty synchronization processes ($\delta = 5°$, 10°, and 30°), the power impulse, the frequency oscillation, and the voltage sag are limited in the network, and the transient stability of faulty synchronization processes is enhanced by the soft-synchronization process with controllable inductive FCLs. The shaft torque impulse is restrained.

Due to the high expense and potential hazard to the equipment, experimental results are not given here. But we offer the parameters of existing FCL equipment and apply them to our simulations in order to validate the proposed scheme.

IV. Conclusion

We have described and characterized a process for soft-synchronization of generators by using controllable inductive

TABLE I
SUMMARY OF SIMULATION RESULTS IN THE SOFT-SYNCHRONIZATION PROCESS IN AN ISOLATED POWER SYSTEM

Rotor-angle Difference, δ	*0°*		*5°*		*10°*		*30°*	
Apply soft-syn. process?	*No*	*Yes*	*No*	*Yes*	*No*	*Yes*	*No*	*Yes*
Max. Frequency Bias (Hz)*	*0.11*	*0.10*	*0.15*	*0.10*	*0.20*	*0.11*	*0.55*	*0.27*
First Peak Power (MW)	*2.6*	*2.8*	*8.6*	*3.9*	*21.3*	*5.5*	*64.9*	*11.2*
Voltage Sag (V)**	-	-	-	-	*50*	-	*259*	*52*

* "Max. Frequency Bias" is the maximum difference between the frequency of *TG1* and the averaged system frequency.
** Mark "-" means: there is no obvious voltage sag.

TABLE II
PARAMETERS OF THE TESTBENCH

Turbo-Generator			
Rated Power	*36 MW*	**Rated Voltage**	*4.16 kV*
Power factor	*0.95 (lagging)*	**Rated frequency**	*60 Hz*
Total inertia	*2.5 s*	**Droop setting**	*4 %*
X_d	*1.81 p.u.*	X_q	*1.76 p.u.*
X_d'	*0.3 p.u.*	X_q'	*0.65 p.u.*
X_d''	*0.23 p.u.*	X_q''	*0.25 p.u.*
T_{d0}'	*8.0 s*	T_{q0}'	*1.0 s*
T_{d0}''	*0.03 s*	T_{q0}''	*0.07 s*
Inductive Fault Current Limiter			
Activation Time	*4 ms*	**Reset Time**	*400 ms*
Maximum inductance	*5 mH*	**Minimum inductance**	*0.1 mH*

FCLs. This soft-synchronization process increases the transient stability margin for faulty synchronizations, and increases the success rate of generator synchronizations under some critical conditions, such as for a low-inertia generator connecting to the grid via a long or high-impedance connection. Also, it limits the power impulse, the amplitude of frequency oscillations, and the voltage sag in power networks during the mistimed synchronization processes, while having no adverse side effects on ideal synchronization processes. Shaft torque impulses are reduced, which should lengthen the life of turbogenerators. This soft-synchronization process can be generally applied to infinite and finite power systems.

APPENDIX

The simulation testbench was implemented in VTB2009 [18]. The gas turbogenerator is modeled after that described in [16] and the full-order synchronous generator model [17]. A synchronization controller [20], [21] and an AVR [22] adjust the shaft speed of the turbine and the magnitude of the excited voltage separately in order to synchronize the turbogenerator set prior to closing it into the network. The FCL parameters are consistent with those of a "Cryo-Pinch" superconducting fault limiter [8], [9]. These models are suitable for the analysis of transient studies of electric power systems.

Each power generating unit has the same structure. The parameters of the testbench are listed in Table II.

REFERENCES

[1] N. K. Fall and B. Marchionini, "Fault current limiter—R&D status and testing issues," presented at the Power Systems Conf. Expo., Seattle, WA, Mar. 2009.

[2] M. Noe and M. Steurer, "High-temperature superconducting fault current limiters: Concepts, applications, and development status," *Superconduct.Sci. Technol.*, vol. 20, pp. R15–R29, 2007.

[3] A. Neumann, "Application of fault current limiters," Dept. Bus. Enterprise Regulatory Reform. London, U.K., 2007. [Online]. Available: www.berr.gov.uk/files/file42656.pdf

[4] S. Patel, K. Stephan, M. Bajpai, R. Das, T. J. Domin, E. Fennell, J. D. Gardell, I. Gibbs, C. Henville, P. M. Kerrigan, H. J. King, P. Kumar, C. J. Mozina, M. Reichard, M. Reichard, J. Uchiyama, S. Usman, D. Viers, D. Wardlow, and M. Yalla, "Performance of generator protection during major system disturbances," *IEEE Trans. Power Del.*, vol. 19, no. 4, pp. 1650–1662, Oct. 2004.

[5] D. A. Tziouvaras and D. Hou, "Out-of-step protection fundamentals and advancements," in *Proc. 57th Annu. Conf. Protective Relay Eng.*, Mar. 30–Apr. 1, 2004, pp. 282–307.

[6] L. C. Gross, L. S. Anderson, and R. C. Young, "Avoid generator and system damage due to a slow synchronizing breaker," in *Proc. 24th Annu. Western Protective Relay Conf.*, Oct. 21–23, 1997, pp. 1–20.

[7] K. Malmedal, P. K. Sen, and J. P. Nelson, "Application of out-of-step relaying for small generators in distributed generation," *IEEE Trans. Ind. Appl.*, vol. 41, no. 6, pp. 1506–1514, Nov./Dec. 2005.

[8] S. B. Kuznetsov, "Method and apparatus for limiting high current electrical faults in distribution networks by use of superconducting excitation in transverse fluux magentic circuit," U.S. Patent No. 5 642 249, Jun. 24, 1997.

[9] S. Kuznetsov, "Apparatus for limiting high current electrical faults in distribution networks by use of superconducting excitation in transverse fluxmagnetic circuit," U.S. Patent No. 5 596 469, Jan. 21, 1997.

[10] S. Lee, C. Lee, T. K. KO, and O. Hyun, "Stability analysis of a power system with superconducting fault current limiter installed," *IEEE Trans. Appl. Superconduct.*, vol. 2, no. 1, pp. 2098–2101, Mar. 2001.

[11] Y. Goto, K. Yukita, K. Mizuno, K. Ichiyanagi, Y. H. Guo, Y. Yokomizu, and T. Matsumura, "Experimental studies on power system transient stability due to introduction of superconducting fault current limiters," in *Proc. IEEE Power Eng. Soc. Winter Meeting*, 2000, pp. 1129–1134.

[12] M. Yagami, S. Shibata, T. Murata, and J. Tamura, "Improvement of power system transient stability by superconducting fault current limiter," in *Proc. IEEE Power Eng. Soc. Transm. Distrib. Asia Pacific Conf. Exhibit.*, 2002, pp. 359–364.

[13] J. R. S. S. Kumara, A. Atputharajah, J. B. Ekanayaka, and F. J. Mumford, "Over current protection coordination of distribution networks with fault current limiters," presented at the IEEE Power Eng. Soc. Gen. Meeting, Montreal, QC, Canada, 2006.

[14] F. J. Mumford and T. W. Preston, "Superconducting fault current limiters—State of the art," in *Proc. VI SEPOPE*, Salvador, Brazil, May 1998, pp. 24–29.

[15] J. L. Rasolonjanahary, J. Sturgess, and E. Chong, "Design and construction of a magnetic fault current limiter," presented at the Ukmag Soc. Meeting, Stamford, U.K., Oct. 12, 2005.

[16] G. A. Putrus, N. Jenkins, and C. B. Cooper, "A static fault current limiting and interrupting devices," in *Inst. Elect. Eng. Colloq. Fault Current Limiters—A Look at Tomorrow*, Jun. 1995, pp. 5/1–5/6, , pp. 5/1–5/6, Jun. 1995.
[17] P. Kundur, *Power System Stability and Control*. Palo Alto, CA: Elect. Power Res. Inst., McGraw-Hill, 1993.
[18] T. Lovett, R. A. Dougal, A. Monti, and E. Santi, "A multilanguage environment for interactive simulation and development of controls for power electronics," in *Proc. IEEE Power Electron. Specialists Conf.*, Vancouver, BC, Canada, 2001, vol. 3, pp. 1725–1729.
[19] W. I. Rowen, "Simplified mathematical representations of heavy-duty gas turbines," *ASME J. Eng. Power*, vol. 105, pp. 865–869, 1983.
[20] Woodward Governor Company, Speed droop and power generation.. Fort Collins, CO, Appl. note 01302. [Online]. Available: http://www.canadiancontrols.com/documents/technical/Speed%20Droop%20and%20Power%20Generation.pdf
[21] M. Andrus, S. Woodruff, and W. Ren, Simulations of islanded generator synchronization in a notional integrated power system. [Online]. Available: http://esrdc.caps.fsu.edu/library.lookup.date.php
[22] P. M. Anderson and A. A. Fouad, *Power System Stability and Control*, 2nd ed. Hoboken, NJ: Wiley, 2002.

Yucheng Zhang (M'10) received the B.S. and M.S. degrees from the College of Electrical and Electronics Engineering, Huazhong University of Science and Technology, Wuhan, China, in 2003 and 2007, respectively, and the Ph.D. degree in electrical engineering from the University of South Carolina, Columbia, in 2010.

Currently, he is a Research Assistant Professor in Electrical Engineering at the University of South Carolina. His previous research focused on power-electronics devices and their applications in electric power systems. His research interests include the protection of power systems as well as electric ship system modeling and analysis.

Roger A. Dougal (SM'94) received the Ph.D. degree in electrical engineering from Texas Tech. University, Lubbock, in 1983.

Currently, he is the Thomas Gregory Professor of Electrical Engineering, University of South Carolina, where he leads the Power and Energy Systems Group. He is a Director of the Electric Ship R&D Consortium, which is developing electric power technologies for the next generation of electric ships. He is Co-Director of the National Science Foundation Industry/University Cooperative Research Center for Grid-Connected Advanced Power Electronic Systems, and he leads development of the Virtual Test Bed—a computational environment for simulation-based-design and virtual prototyping of dynamic, multidisciplinary systems. His research interests include power electronics, hybrid power sources, and simulation methods.